

Ion-pair formation in the photodissociation of HCl and DCl

Andrew J. Yencha^{a)} and Devinder Kaur^{b)}

Department of Chemistry, State University of New York at Albany, Albany, New York 12222

Robert J. Donovan

Department of Chemistry, University of Edinburgh, Edinburgh EH9 3JJ, United Kingdom

Agust Kvaran

Science Institute, University of Iceland, Dunhaga 3, 107 Reykjavik, Iceland

Andrew Hopkirk

SERC Daresbury Laboratory, Daresbury, Warrington WA4 4AD, United Kingdom

H. Lefebvre-Brion and F. Keller

Laboratoire de Photophysique Moléculaire, Université de Paris-Sud, 91405 Orsay, France

(Received 6 April 1993; accepted 22 June 1993)

The vibrationally resolved excitation functions for Cl^- formation from jet-cooled HCl and DCl, following photoabsorption in the region 75–86 nm ($\text{HCl/DCl} + h\nu \rightarrow \text{H}^+/\text{D}^+ + \text{Cl}^-$), are reported and compared with *ab initio* calculations. This completes our understanding of the various possible decay channels available to superexcited states of HCl and DCl that lie above the first ionization limit. Our experimental and theoretical results suggest that the Rydberg states responsible for ion-pair formation in HCl and DCl via predissociation by the $V^1\Sigma^+$ ion-pair state correspond to $^1\Sigma^+$ states that are only weakly autoionized. These same Rydberg states appear to act as, at least, one class of precursor states for neutral dissociation to yield excited H^* and Cl^* atoms.

I. INTRODUCTION

The vacuum-ultraviolet (VUV) photoabsorption, photodissociation, and photoionization spectra of HCl have been extensively studied.^{1–16} These studies have attracted considerable theoretical interest and a broad understanding of the excited states involved is emerging.^{17–23} Above the first two ionization thresholds ($X^2\Pi_{3/2}$ and $X^2\Pi_{1/2}$ at 97.27 and 96.68 nm, respectively), a number of processes can compete and multichannel interactions become important.^{12,21,22} Photodissociation processes to yield excited states of both hydrogen and chlorine atoms have been studied in some detail,^{12,13,22} and these studies are of importance to the present work. The threshold for ion-pair formation ($\text{H}^+ + \text{Cl}^-$) lies at 86.01 nm, however, ion-pair formation from HCl has not previously been observed.

Of particular importance to the present study is the work of Berkowitz *et al.*²⁴ on ion-pair formation from HF. They observed an intense, sharp, $\text{H}^+ (+\text{F}^-)$ peak at 77.19 nm, slightly above the ion-pair threshold at 77.72 nm, followed by weaker and broader bands extending to shorter wavelengths. The ion-pair excitation functions reported here for HCl and DCl are similar to that observed for HF, and we suggest that ion-pair formation occurs by a similar mechanism in all these systems. We also attempted to observe ion-pair formation from HBr and HI but were unsuccessful. Possible reasons for this are discussed.

II. EXPERIMENT

The molecular beam apparatus used in this study and the method for producing positive and negative ion photoexcitation mass spectra have been described in detail previously,^{25–27} so only a brief report will be given here. The results presented here were obtained using beam line U11 of the National Synchrotron Light Source (NSLS) facility of the Brookhaven National Laboratory.

Synchrotron radiation emanating from the NSLS storage ring of 0.09 nm bandpass resolution [full-width at half-maximum (FWHM)] intersected a supersonic beam made up of a mixture of 5% HCl or DCl in He. The molecular beam was generated by passing the gas mixture through a glass nozzle of 200 μm diam then through a 1 mm diam skimmer located 5–10 mm downstream. The pressure in the nozzle was adjusted to obtain the maximum mass-selected ion intensity. Typically, this was achieved at ~ 190 Torr, as measured on a capacitance manometer. Similar conditions were used in the HBr and HI studies. The HCl gas used in this study was purchased from Matheson Gas Products Co. (East Rutherford, NJ) and was of so-called semiconductor purity, while the DCl gas used was purchased from Merck, Sharp, and Dohme (Montreal, Quebec) of stated purity 99+ % DCl. Both gases were used directly.

III. RESULTS AND DISCUSSION

The excitation spectra for Cl^- formation from HCl and DCl are shown in Fig. 1 as the middle and bottom traces, respectively. The thermodynamic thresholds for ion-pair formation in HCl and DCl are at 86.01 and 85.70 nm, respectively, as marked in Fig. 1. These values were

^{a)}Also Department of Physics, State University of New York at Albany.

^{b)}Present address: Laporte Industries Pte. Ltd. 14 Tunas Ave. 20 Singapore 2263.

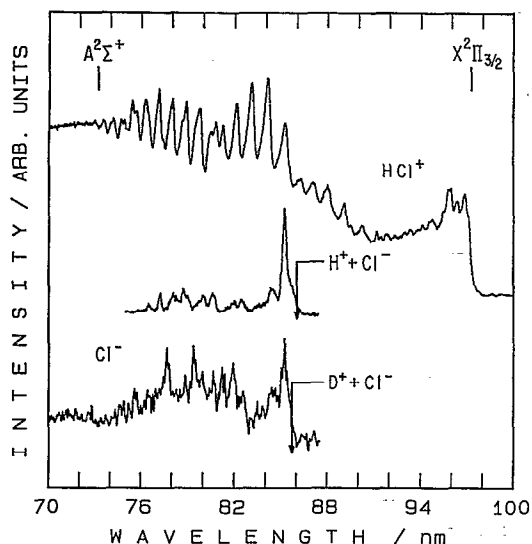


FIG. 1. Excitation functions for Cl^- formation from HCl (middle trace) and from DCl (bottom trace) together with the ionization function for the parent molecule, HCl (top trace). The thermodynamic thresholds for formation of the ion pairs $\text{H}^+(^1S_0) + \text{Cl}^-(^1S_0)$ and $\text{D}^+(^1S_0) + \text{Cl}^-(^1S_0)$ and for formation of the parent ion, $\text{HCl}^+(X^2\Pi_{3/2}, A^2\Sigma^+)$, are indicated.

derived from $D_0(\text{HCl})=4.4336$ eV,²⁸ $D_0(\text{DCl})=4.4852$ eV,²⁸ $\text{IP}(\text{H,D})=13.598$ eV,²⁹ and $\text{EA}(\text{Cl})=3.617$ eV,³⁰ and the use of the conversion factor³¹ 1 eV = 8065.541 cm^{-1} . The two excitation functions are very similar, but the Cl^- spectrum from DCl is considerably noisier due to the lower signal strength (estimated to be about one-half of that of Cl^- from HCl). The difference in Cl^- signal strength between HCl and DCl, which is not predicted theoretically (see below), may be due to a difference in collection efficiency for the different kinetic energies of Cl^- produced in the photodissociation process. It is noteworthy that, in general, the peaks in the DCl spectrum are sharper than those in the HCl spectrum, which may reflect a more efficient rotational cooling in DCl in the jet expansion. A striking feature in these spectra is the intense, sharp peak, just above threshold, at 85.22 nm, as seen in both spectra (see also column 2 in Tables I and II). This region of the excitation spectra strongly resembles that for $\text{H}^+ (+\text{F}^-)$ formation from HF, reported by Berkowitz *et al.*²⁴ Also shown in Fig. 1 (top trace) is the ionization efficiency curve for HCl. The positions of the ionization potentials for HCl are marked in Fig. 1 for reference; they are $\text{HCl}^+(X^2\Pi_{3/2})=97.27$ nm (Ref. 32) and $\text{HCl}^+(A^2\Sigma^+)=73.19$ nm.³³ Pronounced autoionization structure is observed that corresponds well with previous reports.^{5,6,13,15,21,34-36} At shorter wavelengths the Cl^- excitation functions differ from that for $\text{H}^+ (+\text{F}^-)$ formation from HF. The latter tails quite rapidly down to the baseline with some superimposed broad structure. The Cl^- excitation functions (see Fig. 1), extend over a much wider region, and the intensity and spacing of the peaks are somewhat irregular. The very intense peak observed in the threshold region for HCl, DCl, and HF contrasts sharply with the broad structure observed to shorter wavelengths.

TABLE I. Measured and calculated peak positions and their assignments in the excitation function of Cl^- from HCl.

Peak number ^a	Measured wavelength ^b (nm)	Calculated wavelength (nm)	Assignment ^c
1S	85.8	85.84	$4s\sigma$ $v=8$
2	85.22	85.29	$4s\sigma$ $v=9$
3	84.40	84.45	$3d\sigma$ $v=9$
4	83.45	83.30	$4p\sigma$ $v=5$
5	82.45	82.79	$4p\sigma$ $v=6$
6	81.97	81.49	$5s\sigma$ $v=2$
7	80.60	80.54	$5s\sigma$ $v=3$
8	79.97		
9S	79.70	79.70	$5s\sigma$ $v=4$
10S	79.00	78.90	$5s\sigma$ $v=5$
11	78.78	78.59	$6s\sigma$ $v=2$
12	78.07	78.28	$5s\sigma$ $v=6$
		77.92	$6s\sigma$ $v=3$
		77.63	$5s\sigma$ $v=7$
13	77.27	77.33	$5s\sigma$ $v=8$
14	76.52	76.73	$6s\sigma$ $v=4$
15	75.81	76.05	$6s\sigma$ $v=5$

^aSee Fig. 4 for identification. The letter S signifies a shoulder.

^bUncertainty = ± 0.09 nm.

^cSee also Fig. 4.

It has been suggested that ion-pair formation in HF proceeded through an initial transition to bound excited (Rydberg) states of the molecule which were, in turn, pre-dissociated into $\text{H}^+ + \text{F}^-$, via the $V^1\Sigma^+$ ion-pair state.²⁴ We have discussed a similar mechanism for ion-pair formation in Br_2 ,²⁵ I_2 ,³⁷ and the interhalogens BrCl , ICl , and IBr .³⁸ It appears that the dominantly involved Rydberg

TABLE II. Measured and calculated peak positions and their assignments in the excitation function of Cl^- from DCl.

Peak number ^a	Measured wavelength ^b (nm)	Calculated wavelength (nm)	Assignment ^c
1S	85.64	85.75	$4s\sigma$ $v=11$
2	85.22	85.24	$4s\sigma$ $v=12$
3	85.00	84.95	$4s\sigma$ $v=13$
4	84.51	84.48	$3d\sigma$ $v=11$
5	83.84	83.63	$4p\sigma$ $v=7$
6	83.47		
7	83.09	83.06	$4d\sigma$ $v=0$
8	82.56	82.63	$4p\sigma$ $v=9$
9	81.92	82.02	$5s\sigma$ $v=2$
10	81.19	81.07	$5s\sigma$ $v=3$
11	80.66	80.49	$5s\sigma$ $v=4$
12	79.96	79.86	$5s\sigma$ $v=5$
13	79.37	79.37	$5s\sigma$ $v=6$
14	78.75	78.76	$5s\sigma$ $v=7$
		78.19	$5s\sigma$ $v=8$
		77.80	$5s\sigma$ $v=9$
15	77.66	77.66	$6s\sigma$ $v=4$
16	77.00	77.03	$6s\sigma$ $v=5$
17	76.53	76.65	$7s\sigma$ $v=2$
18	75.67	76.41	$6s\sigma$ $v=6$

^aSee Fig. 5 for identification. The letter S signifies a shoulder.

^bUncertainty = ± 0.09 nm.

^cSee also Fig. 5.

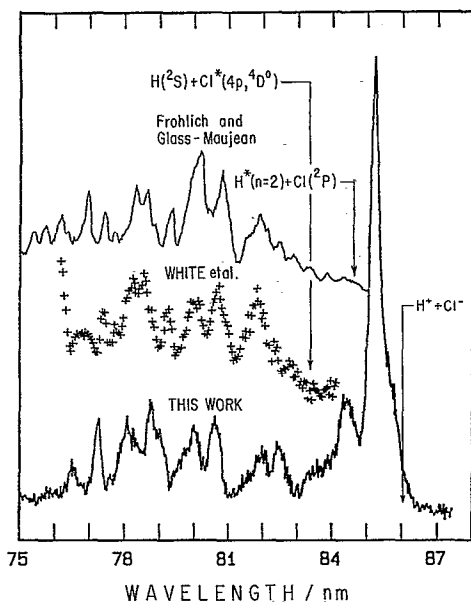


FIG. 2. Comparison of the excitation functions for Cl^- formation from HCl (bottom trace) with the fluorescence excitation functions for H^* and Cl^* production measured by Frohlich and Glass-Maujean (Ref. 13) (top trace) and by White *et al.* (Ref. 12) (middle trace), respectively. The thermodynamic thresholds for formation of the ion pairs $\text{H}^+(^1S_0) + \text{Cl}^-(^1S_0)$ and for formation of the excited neutrals $\text{H}^*(n=2) + \text{Cl}(3p^5, ^2P)$ and $\text{H}(^2S) + \text{Cl}(4p, ^4D^0)$ are indicated.

states in diatomic halogen systems are of (0^+) symmetry that are homogeneously predissociated by a (0^+) valence, ion-pair state via electrostatic coupling. Here, we propose that the excited states involved in Cl^- formation in HCl and DCl are $^1\Sigma^+$ Rydberg states with an $A^2\Sigma^+$ core.

The initial sharp peak in the Cl^- excitation function from HCl observed here at 85.22 nm (see the middle trace in Fig. 1) coincides in peak position (but not shape) with the autoionizing peak in the photoionization efficiency curve of HCl shown in the top trace of Fig. 1. However, this correspondence is purely accidental, because this autoionizing peak has been assigned to a $^1\Pi$ Rydberg state^{21,22} which we have determined would yield a very small photodissociation cross section through heterogeneous rotational coupling with the $V^1\Sigma^+$ ion-pair state.³⁹ The weaker Cl^- structure between 75 and 85 nm shown in Fig. 1 appears quite similar to the neutral dissociative fluorescence excitation spectra reported by White *et al.*¹² and Frohlich and Glass-Maujean¹³ (see Fig. 2), thus suggesting similar intermediate "doorway" Rydberg states in the three dissociative processes as described below. Variations in intensity and width of the peak structure as displayed in Fig. 2 can be accounted for on the basis of differences in the coupling of the bound Rydberg states to the various continuum exit channels observed in the three experiments. In the study of White *et al.*,¹² the fluorescence wavelength detected was limited to the range 180–850 nm. They concluded that the total fluorescence detected in the excitation region 77–84 nm to be due to excited Cl^* atoms with a $3p^4(^3P)4p$ configuration. Based on the possible dissociative channels in this excitation range and detectable in

their experiment, the longest wavelength threshold occurs at 83.39 nm,¹² $\text{H}(^2S) + \text{Cl}^*(4p, ^4D^0)$, and is indicated in Fig. 2. In the experimental setup used by Frohlich and Glass-Maujean,¹³ fluorescence from $\text{H}^*(n=2)$ and $\text{Cl}^*(3p^4s, ^2P$ or $^4P)$ fragments could be detected, placing the longest wavelength threshold below 85 nm at 84.74 nm,¹² $\text{H}^*(n=2) + \text{Cl}(3p^5, ^2P)$, as so indicated in Fig. 2. In both of these cases, fluorescence appears to begin at or near threshold and builds towards shorter wavelengths. Thus, it would seem that both exit channels are active in the excitation spectra as represented by the authors.^{12,13} In a related study of HCl,⁴⁰ the presence of the excited fragment atoms, $\text{H}^*(n=2)$ and $\text{Cl}^*(4s, ^2P)$, were positively confirmed by measuring the photoelectron spectrum obtained by $(2+1)$ resonance enhanced multiphoton (REMP) excitation to populate the dissociative superexcited states of HCl, followed by ionization of the excited fragment species by the absorption of an additional photon. In another $(2+1)$ REMF excitation study of HCl,⁴¹ the dissociative exit channels $\text{H}^*(n=2) + \text{Cl}(3p^5, ^2P)$ and $\text{H}(^2S) + \text{Cl}^*(4p, ^4P)$ were detected slightly above their onset energies in the following way. The $v'=3$ and 4 levels of the $V^1\Sigma^+$ ion-pair state were populated by two-photon absorption and used to access the respective dissociative state by the absorption of a third photon. Detection of the excited-state species, H^* and Cl^* , was made by the appearance of H^+ and Cl^+ by the absorption of an additional photon by the respective excited fragment atom. Lefebvre-Brion and Keller²² have interpreted predissociation in HCl producing Cl^* in terms of both $^1\Sigma^+$ and $^1\Pi$ Rydberg states with an $A^2\Sigma^+$ core predissociated by repulsive states converging to the repulsive $a^4\Pi$ state of HCl^+ . Frohlich and Glass-Maujean¹³ assigned their HCl dissociative fluorescence excitation spectrum in the 73–85 nm range (see their Fig. 7) to several overlapping $^1\Sigma^+$ and $^3\Pi$ Rydberg states, the latter being dominant in their spectrum. Note that the rate of predissociation for the mechanism invoked by these authors would be at least one order of magnitude less than the rate of predissociation for our proposed mechanism.⁴²

The question is, what Rydberg states are involved in the predissociation in HCl/DCl to produce ion pairs? The high vibrational levels of Rydberg states with a $X^2\Pi$ core are lying in the wavelength range encompassing the Cl^- excitation function (75–86 nm), but these levels cannot be excited from the ground state due to the very small Franck-Condon factors implied in the transition. We propose that the states are $^1\Sigma^+$ Rydberg states with an $A^2\Sigma^+$ core. Following Table III of Ref. 12, the dissociation products giving $^1\Sigma^+$ Rydberg states are successively, $\text{H}^*(n=2) + \text{Cl}(3p^5, ^2P)$ at 84.74 nm that we correlate to the $4s\sigma$ state, in agreement with the order of Rydberg states calculated previously,²¹ $\text{H}(^2S) + \text{Cl}^*(4s, ^2D)$ at 84.32 nm, correlated to the $3d\sigma$ state, $\text{H}(^2S) + \text{Cl}^*(4p, ^2P)$ at 82.51 nm, correlated to the $4p\sigma$ state, and $\text{H}(^2S) + \text{Cl}^*(4p', ^2P)$ at 76.86 nm, correlated to the $5s\sigma$ state. The $6s\sigma$ curve has been taken to be parallel to the $5s\sigma$ curve. To aid in visualizing the interactions taking place in photoexcitation of HCl above the lowest ionization limit resulting in dissociative ion-pair formation and neutral dissociative fluorescence,

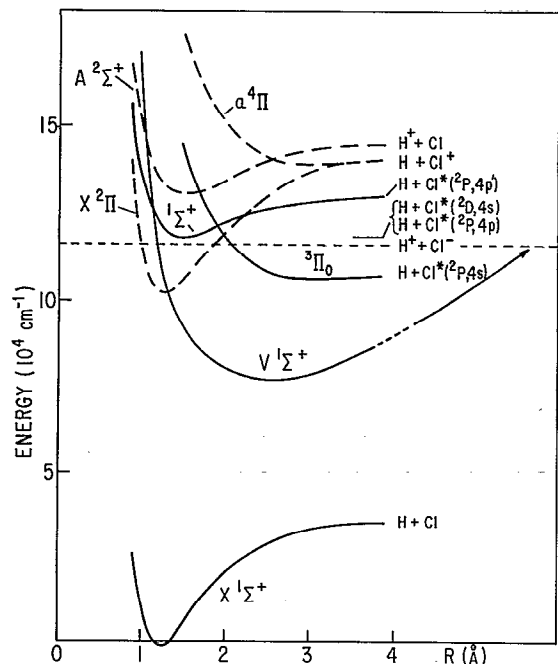


FIG. 3. Selected semiexperimental potential curves for HCl/HCl⁺ adapted from Fig. 6 of Ref. 22. The RKR potential curve for the $V^1\Sigma^+$ state was obtained from Frohlich. The $(5s\sigma)^1\Sigma^+$ curve is shown being crossed on the right by the $^3\Pi_0$ curve, leading to dissociation into neutral atoms, and on the left by the $V^1\Sigma^+$ curve, leading to dissociation into ion pairs.

we present in Fig. 3 selected semiexperimental potential curves for the HCl/HCl⁺ system, including a representative $^1\Sigma^+$ Rydberg curve ($5s\sigma$) converging on the HCl⁺ $^2\Sigma^+$ ion, the $V^1\Sigma^+$ ion-pair curve, and a $^3\Pi_0$ repulsive curve converging on the $a^4\Pi$ HCl⁺ ion. The asymptotic limits for two additional $^1\Sigma^+$ Rydberg states yielding excited chlorine atoms, as given above, are also shown. The $^1\Sigma^+$ Rydberg state dissociating to the excited hydrogen atom plus the ground-state chlorine atom mentioned above is not shown for clarity. It can be seen in Fig. 3 that the $(5s\sigma)^1\Sigma^+$ curve is crossed on the right by the $^3\Pi_0$ curve, leading to dissociation into neutral atoms, and on the left by the $V^1\Sigma^+$ curve, leading to dissociation into ion pairs.

To test the proposition that $^1\Sigma^+$ Rydberg states are responsible for ion-pair formation in photoexcitation of HCl and DCl, *ab initio* calculations were performed that were used to derive simulated photodissociative ion-pair excitation spectra for both HCl and DCl, in the following manner. It was assumed that the bottom of the potential curves of the $^1\Sigma^+$ Rydberg states run parallel to the curve of the $A^2\Sigma^+$ ion state (see Fig. 3) with the different dissociation limits as given above. Then, Franck-Condon factors for transitions from the ground state of HCl/DCl to these Rydberg states were computed in the standard numerical way. The $V^1\Sigma^+$ ion-pair state was represented by a Rydberg-Klein-Rees (RKR) potential with an asymptotic ionic behavior. This ionic behavior was taken into account in the calculations of the vibrational continuum wave function of this state. At smaller internuclear distances, the $V^1\Sigma^+$ potential curve was slightly adjusted in

order to reproduce the experimental variation of the peak intensities with energy due to the overlap between vibrational bound and continuum levels. The inner crossing point of the $V^1\Sigma^+$ potential with the $^1\Sigma^+$ Rydberg state potential is responsible for the position of the intensity maximum in the vibrational progression of the dissociation spectrum. It has been adjusted to reproduce the intensity maximum of the $ns\sigma$ progression in the 78–80 nm wavelength range. The electronic interactions between the $^1\Sigma^+$ Rydberg states and the $V^1\Sigma^+$ ion-pair state have an electrostatic origin. These interactions have been estimated by performing *ab initio* calculations, with and without diffuse orbitals, because the electronic configurations involved differ by only one orbital. The electronic interaction between the $V^1\Sigma^+$ and the $4s\sigma$ states is the strongest, and has been found to be equal to 7000 cm⁻¹. The interactions between the other $ns\sigma$ states must be weighted by the $n^{*-3/2}$ factor. For the $3d\sigma$ and $4p\sigma$ Rydberg states, the electronic interactions are weaker and have been taken equal to 300 and 700 cm⁻¹, respectively, slightly different from the *ab initio* values of 550 and 450 cm⁻¹, respectively. We introduced the $s\sigma$, $p\sigma$, and $d\sigma$ Rydberg states with quantum defects 1.90, 1.55, and 0.83, respectively, all of which were both predissociated by the $V^1\Sigma^+$ ion-pair state and autoionized by the $X^2\Pi$ HCl⁺ continuum. The transition moments for the Rydberg states and the interaction of the Rydberg states with the ionization continuum of $X^2\Pi$ have been taken from Ref. 21, the latter of which have been multiplied by a factor of 2 for $s\sigma$ and $d\sigma$ states and by a factor of $2^{1/2}$ for $p\sigma$ states in order to try to reproduce the observed broad widths of the experimental bands.

With all these parameters, we have performed a multichannel quantum defect theory (MQDT) calculation, using a program written previously.²² The same parameters were taken for both HCl and DCl; only the reduced mass was changed. The results of these calculations for HCl and DCl gave the photodissociative cross section spectra for ion-pair formation resulting from different Rydberg series. They were convoluted to the experimental bandpass resolution equal to 0.09 nm. These spectra are shown in the upper portion of Figs. 4 and 5, respectively, where they are compared with the experimental Cl⁻ excitation function spectra. The calculated peak wavelength positions, which actually correspond to a superposition of several Rydberg peaks belonging to different Rydberg series, are given in column 3 in Tables I and II, respectively, where they are compared with the experimentally derived peak positions (column 2). Also given in Tables I and II, in column 4, are the assignments of the most important contribution of the peaks listed in column 3 of these tables. The Rydberg series assignments are also shown in the upper portion of Figs. 4 and 5, where it can be seen that some of the vibrational spacings appear irregular due to the superposition of several Rydberg bands.

From an inspection of the spectral results presented in Figs. 4 and 5, it is clear that there is a good qualitative agreement between the calculated and observed photodissociation spectra, and the numerical data given in Tables I and II indicate a good quantitative correspondence. The

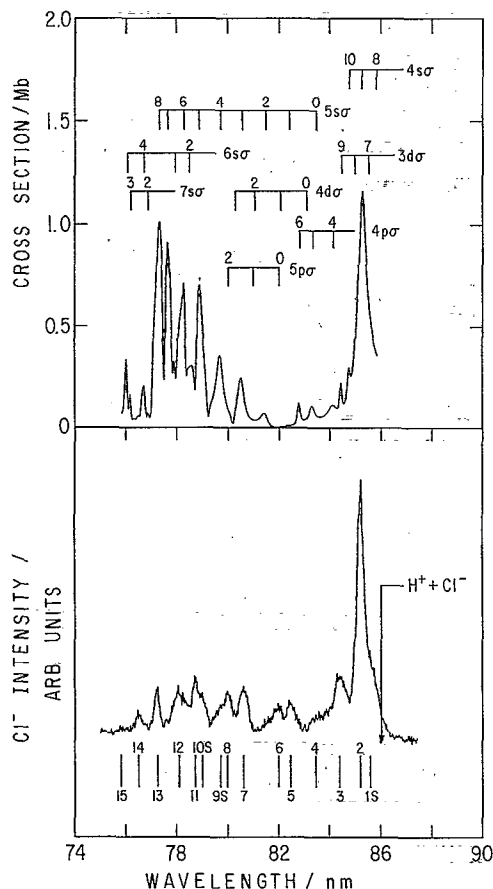


FIG. 4. Comparison of the experimental excitation function for Cl^- formation from HCl (lower trace) with the calculated cross section for ion-pair formation in HCl (upper trace). The peak numbers in the lower portion of the figure refer to the experimental Cl^- excitation function, the wavelength positions of which are listed in column 2 in Table I. The assignment of the Rydberg series obtained from the calculated spectrum are shown in the upper portion of the figure and listed in column 4 in Table I. The thermodynamic threshold for the formation of ion pairs $\text{H}^+(^1S_0) + \text{Cl}^-(^1S_0)$ is indicated.

agreement in the line positions is not at all fortuitous, because the line positions are strongly dependent on the choice of the calculation parameters. We emphasize that the same set of parameters have been used for both HCl and DCl. Furthermore, the number of $^1\Sigma^+$ Rydberg states lying in the energy region is limited by the restricted number of allowed dissociation limits. These facts support the assignment of the precursor Rydberg states to $^1\Sigma^+$ states. However, there are some differences that can be noted in the spectral findings. Namely (1) there appears to be an underlying background in the Cl^- excitation functions in HCl/DCl that does not appear in the calculated spectra. This is possibly due to a presence of a quasicontinuum background as a result of the direct populating of the $V^1\Sigma^+$ state from the ground state of HCl/DCl that was not included in the derivation of the calculated spectra. (2) The relative intensity profile in the 80–84 nm region is not adequately represented in the calculated spectra. This may be due to the opening up of the competitive neutral dissociative excitation channels in this wavelength region as de-

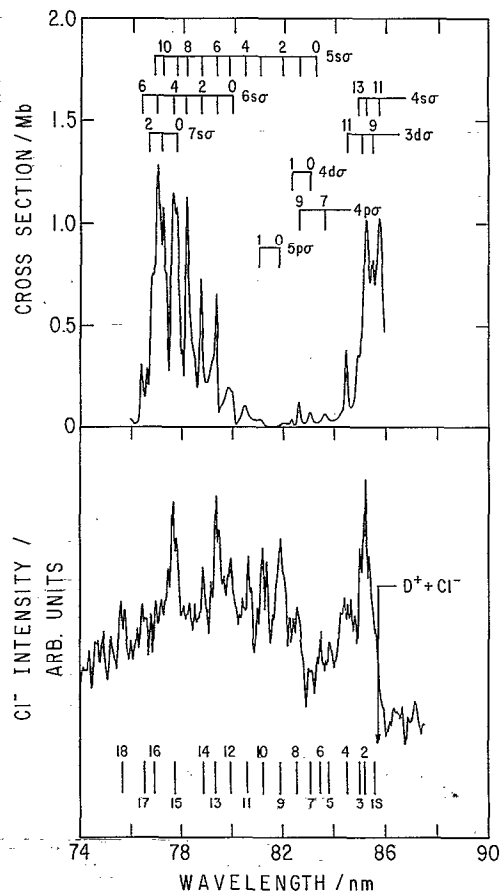


FIG. 5. Same as in Fig. 4, except for DCl. Reference is made to Table II.

scribed above, that was likewise not included in the current MQDT treatment. Although the opening up of a new channel cannot directly enhance the intensity of the ion-pair dissociation spectra, the solution of the multichannel problem can be different from the sum of the solutions for each individual channel. A full theoretical study incorporating both of the above effects is currently underway.

We have also attempted to observe ion-pair formation from HBr and HI, but were unsuccessful. The yield of Br^- and I^- from HBr and HI, respectively, must be $< 10^{-1}$ of that for Cl^- from HCl, based on our estimated experimental detection limits. This is most likely due to the following. For heavier molecules, the electrostatic interaction is probably weaker, as usual, and consequently, the dissociation into ion pairs becomes less favorable. In addition, the spin-orbit interaction responsible for dissociation into neutral atoms becomes larger and larger. For example, for HBr the spin-orbit interaction has been calculated to be four times larger than in HCl, at least at low excitation energy.⁴³ For HI, it is expected to be also a factor of 4 times greater than in HBr.⁴²

In conclusion, ion-pair formation in HCl and DCl has been detected for the first time in the 75–86 nm region, which appears, based on *ab initio* calculations, to be associated with the populating of several $^1\Sigma^+$ Rydberg states ($ns\sigma$, $np\sigma$, and $nd\sigma$) converging on the $A^2\Sigma^+$ ion that are electrostatically coupled to the $V^1\Sigma^+$ ion-pair state lead-

ing to dissociation. These same Rydberg states in the 75–85 nm region appear to be competitively coupled to dissociative neutral molecular states resulting in both $H^*(n=2)$ and $Cl^*(4p)$ fluorescence. The similarity between the ion-pair structure observed in HCl and HF is perhaps fortuitous, because in the case of HF, probably, the Rydberg states with a $X^2\Pi$ core play an important role, and there are now Rydberg states with an $A^2\Sigma^+$ core with low vibrational levels which lie in the energy region just above the $H^+ + F^-$ dissociation limit.

A different point of view of dissociation in HCl, based on an adiabatic approach, in the energy region above the ion-pair dissociation limit that could account for the neutral and ionic spectral results presented in Fig. 2 is as follows. Photoexcitation from the ground state of HCl occurs to quasibound $^1\Sigma^+$ Rydberg states of mixed Rydberg/ion-pair continuum character. The Franck–Condon factors for the excitation may be viewed as the Franck–Condon factors for transitions to a pure, unperturbed $^1\Sigma^+$ Rydberg state augmented by the admixture of ion-pair continuum character. This is completely analogous to the situation repeatedly found in the excitation/de-excitation properties of the halogen and interhalogen systems in the energy region approaching the lowest ionization limit in these molecules.^{44–51} The situation in Cl_2 is the exception, where the ion-pair dissociation limit lies above the lowest ionization potential of Cl_2 ,⁵² thus it is analogous to the halogen acid cases, except for HF. The only difference is the energy positioning of the ion-pair state relative to accessible Rydberg states. That is, the interactions (Rydberg/ion-pair) are quite the same.

Once these mixed $^1\Sigma^+$ Rydberg/ion-pair continuum states are populated in HCl, there are five recognizable de-excitation routes that can be identified. The first is that of radiative decay, but this is apparently very improbable in halogen systems where competing processes seem to dominate. For example, there are no known cases where de-excitation from any Rydberg states back to the ground state has been detected in the VUV spectral region following photoexcitation in halogen systems. A second decay route for mixed Rydberg/ion-pair continuum states of $^1\Sigma^+$ symmetry would be via electrostatic autoionization to produce $HCl^+(X^2\Pi_i)$. It has been determined that this is of relatively lesser importance as a decay mechanism in HCl as compared with autoionization of $^1\Pi$ states,²² but nevertheless is of a substantial magnitude as compared with the dissociative processes considered here. The three remaining decay mechanisms in HCl are those responsible for the spectral results presented in Fig. 2, which appear to be of comparable importance. Namely, predissociation of the mixed $^1\Sigma^+$ Rydberg/ion-pair continuum states to produce the neutral fragments in the two channels, $H + Cl^*$ and $H^* + Cl$, and relaxation of the Rydberg/ion-pair continuum states into the ion-pair continuum. The first neutral dissociation channel ($H + Cl^*$) occurs by means of curve crossings of the $^3\Pi_0$ repulsive state with the outer limb of the mixed Rydberg/ion-pair continuum states. This occurs by a spin-orbit interaction mechanism.²² The second neutral dissociation channel ($H^* + Cl$) results from the so-

called indirect (or accidental) predissociation mechanism⁵³ that we believe occurs between two mixed Rydberg/continuum states of the same $^1\Sigma^+$ symmetry lying in the same energy region—one quasibound (the entrance state) and one dissociative (the exit state)—that interact with one another electrostatically. From the spectral results presented in Fig. 2 and the computational results presented here, these dissociative processes are of comparable cross sectional magnitudes and account for up to ~9% of the energy utilization in the 75–86 nm range in HCl, e.g., $(4 + 1 + 1) \text{ Mb} / (63 + 6) \text{ Mb} \cong 0.087$. That is, where the numerator represents the cross sections for the three dissociative channels (i.e., $H^* + Cl$,¹³ $H + Cl^*$,²² and $H^+ + Cl^-$, respectively), and where the denominator is the total photoexcitation cross section (i.e., the sum of direct ionization + autoionization of $^1\Pi$ and $^1\Sigma^+$ Rydbergs¹³ and dissociation into three channels). This finding is found to be consistent with the conclusion drawn earlier²² regarding the relative magnitude of photodissociative processes in HCl.

ACKNOWLEDGMENTS

A.J.Y. thanks the Brookhaven National Laboratory for the use of the NSLS facility and Dr. J. R. Grover and Dr. M. G. White for their helpful advice and assistance in carrying out these experiments and for their hospitality. A.J.Y. also thanks Dr. K. P. Lawley for many stimulating discussions. Dr. C. J. Barbero's assistance in helping collect the DCl mass spectral data is sincerely appreciated. H.L.B. and F.K. thank Dr. H. Fröhlich for supplying the RKR potential curve for the $V^1\Sigma^+$ state of HCl. A.J.Y. gratefully acknowledges the partial support of these studies by a State University of New York at Albany (SUNYA) faculty research fellowship grant, a SUNYA Office for Research grant, and a NSLS Faculty/Student research grant. A NATO travel grant (No. 870878) was instrumental in the collecting of the experimental data presented in this paper.

¹W. C. Price, Proc. R. Soc. London, Ser. A **167**, 216 (1938).

²S. G. Tilford, M. L. Ginter, and J. T. Vanderslice, J. Mol. Spectrosc. **33**, 505 (1969).

³S. G. Tilford and M. L. Ginter, J. Mol. Spectrosc. **40**, 568 (1971).

⁴J. A. Myer and J. A. R. Samson, J. Chem. Phys. **52**, 266 (1971).

⁵D. T. Terwilliger and A. L. Smith, J. Mol. Spectrosc. **45**, 366 (1973).

⁶D. T. Terwilliger and A. L. Smith, J. Chem. Phys. **63**, 1008 (1975).

⁷E. C. Y. Inn, J. Atmos. Sci. **32**, 2375 (1975).

⁸A. E. Douglas and F. R. Greening, Can. J. Phys. **57**, 1650 (1979).

⁹P. L. Smith, K. Yoshino, J. H. Black, and W. H. Parkinson, Astrophys. J. **238**, 874 (1980).

¹⁰D. S. Ginter and M. L. Ginter, J. Mol. Spectrosc. **90**, 177 (1981).

¹¹J. B. Nee, M. Sato, and L. C. Lee, J. Chem. Phys. **85**, 719 (1986).

¹²M. G. White, G. E. Leroi, M.-H. Ho, and E. D. Poliakov, J. Chem. Phys. **87**, 6553 (1987).

¹³H. Fröhlich and M. Glass-Maujean, Phys. Rev. A **42**, 1396 (1990).

¹⁴H. Fröhlich, P. M. Guyon, and M. Glass-Maujean, J. Chem. Phys. **94**, 1102 (1991).

¹⁵M. Krauss, J. A. Walker, and V. H. Diebler, J. Res. Natl. Bur. Stand. US **72**, 281 (1968).

¹⁶P. M. Dehmer and W. A. Chupka, Argonne National Laboratory Report No. ANL-78-65, 1978, p. 13.

¹⁷J. Raftery and W. G. Richards, J. Phys. B **6**, 1301 (1973).

¹⁸M. Bettendorff, S. D. Peyerimhoff, and R. J. Buenker, Chem. Phys. **66**, 261 (1982).

- ¹⁹E. F. van Dishoeck and M. C. van Hermert, *J. Chem. Phys.* **77**, 3693 (1982).
- ²⁰S. C. Giverty and G. C. Balint-Kurti, *J. Chem. Soc. Faraday Trans.* **82**, 1231 (1986).
- ²¹H. Lefebvre-Brion, P. M. Dehmer, and W. A. Chupka, *J. Chem. Phys.* **88**, 811 (1988).
- ²²H. Lefebvre-Brion and F. Keller, *J. Chem. Phys.* **90**, 7176 (1989).
- ²³W. von Niessen, P. Tomasello, J. Schirmer, L. S. Cederbaum, R. Cambi, F. Tarantelli, and A. Sgamellotti, *J. Chem. Phys.* **92**, 4331 (1990).
- ²⁴J. Berkowitz, W. A. Chupka, P. M. Guyon, J. H. Holloway, and R. Spohr, *J. Chem. Phys.* **54**, 5165 (1971).
- ²⁵A. J. Yencha, D. K. Kela, R. J. Donovan, A. Hopkirk, and A. Kvaran, *Chem. Phys. Lett.* **165**, 283 (1990).
- ²⁶M. G. White and J. R. Grover, *J. Chem. Phys.* **79**, 4124 (1983).
- ²⁷J. R. Grover, E. A. Walters, J. K. Newman, and M. G. White, *J. Am. Chem. Soc.* **107**, 7329 (1985).
- ²⁸K. P. Huber and G. Herzberg, *Constants of Diatomic Molecules* (Van Nostrand, Princeton, 1979).
- ²⁹C. E. Moore, *Natl. Stand. Ref. Data Ser. Natl. Bur. Stand.* **34** (1970).
- ³⁰H. Hotop and W. C. Lineberger, *J. Phys. Chem. Ref. Data* **14**, 731 (1985).
- ³¹E. R. Cohen and B. N. Taylor, *J. Phys. Chem. Ref. Data* **17**, 1795 (1988).
- ³²R. G. Tonkyn, R. T. Weidmann, and M. G. White, *J. Chem. Phys.* **95**, 3696 (1992).
- ³³H. Hotop, G. Hubler, and L. Kaufhold, *Int. J. Mass Spectrom. Ion Phys.* **17**, 163 (1975).
- ³⁴T. A. York and J. Comer, *J. Phys. B* **17**, 2563 (1984).
- ³⁵R.-G. Wang, M. A. Dillon, and D. Spence, *J. Chem. Phys.* **80**, 63 (1984).
- ³⁶D. Shaw, D. Cvejanovic, G. C. King, and F. H. Read, *J. Phys. B* **17**, 1173 (1984).
- ³⁷A. Kvaran, A. J. Yencha, D. K. Kela, R. J. Donovan, and A. Hopkirk, *Chem. Phys. Lett.* **179**, 263 (1991).
- ³⁸D. Kaur, A. J. Yencha, R. J. Donovan, A. Kvaran, and A. Hopkirk, *Org. Mass Spectrom.* **28**, 327 (1993).
- ³⁹The ${}^1\Pi$ Rydberg state and the $V{}^1\Sigma^+$ valence state can have an interaction by rotational coupling because their configurations ($A{}^2\Sigma^+$) $3d\pi$ and ($A{}^2\Sigma^+$) σ^* , respectively, differ by only one orbital, but the matrix element of this operator, between the valence and Rydberg orbitals, would be negligible. In addition, these states could also interact indirectly through the intermediate ${}^1\Sigma^+$ Rydberg state, with the configuration ($A{}^2\Sigma^+$) $3d\sigma$; the matrix element being given by the expression $\langle V{}^1\Sigma^+ | H_{el} | {}^1\Sigma^+ 3d\sigma \rangle \langle {}^1\Sigma^+ 3d\sigma | B | + | {}^1\Pi 3d\pi \rangle [J(J+1)]^{1/2} / [E({}^1\Sigma^+) - E({}^1\Pi)]$. However, using the values of the interactions given later on in this paper, the ratio of this indirect interaction to that of the direct one, $\langle V{}^1\Sigma^+ | H_{el} | {}^1\Sigma^+ 4s\sigma \rangle$, is only $\sim 3 \times 10^{-4}$ (for $J=4$).
- ⁴⁰E. de Beer, B. G. Kocinders, M. P. Koopmanns, and C. A. de Lange, *J. Chem. Soc. Faraday Trans.* **86**, 2035 (1990).
- ⁴¹D. S. Green and S. C. Wallace, *J. Chem. Phys.* **96**, 5857 (1992).
- ⁴²H. Lefebvre-Brion, in *AIP Conf. Proc.* **225**, 275 (1991).
- ⁴³H. Lefebvre-Brion, M. Salzmann, H. W. Klausung, M. Müller, N. Bowering, and U. Heinzmann, *J. Phys. B* **22**, 3891 (1989).
- ⁴⁴A. Hiraya, K. Shobatake, R. J. Donovan, and A. Hopkirk, *J. Chem. Phys.* **88**, 52 (1987).
- ⁴⁵D. I. Austin, R. J. Donovan, A. Hopkirk, K. P. Lawley, D. Shaw, and A. J. Yencha, *Chem. Phys.* **118**, 91 (1987).
- ⁴⁶A. J. Yencha, R. J. Donovan, A. Hopkirk, and D. Shaw, *J. Phys. Chem.* **92**, 5523 (1988).
- ⁴⁷A. Hopkirk, D. Shaw, R. J. Donovan, K. P. Lawley, and A. J. Yencha, *J. Phys. Chem.* **93**, 7338 (1989).
- ⁴⁸K. P. Lawley, E. A. Kerr, R. J. Donovan, A. Hopkirk, D. Shaw, and A. J. Yencha, *J. Phys. Chem.* **94**, 6201 (1990).
- ⁴⁹A. J. Yencha, T. Ridley, R. Maier, R. V. Flood, K. P. Lawley, R. J. Donovan, and A. Hopkirk, *J. Phys. Chem.* **97**, 4582 (1993).
- ⁵⁰S. D. Peyerimhoff and R. J. Buenker, *Chem. Phys.* **57**, 279 (1981).
- ⁵¹T. Moeller, B. Jordan, P. Gürtler, G. Zimmerer, D. Haaks, J. le Calvé, and M. Castex, *Chem. Phys.* **76**, 295 (1983).
- ⁵²J. Berkowitz, C. A. Mayhew, and B. Ruscic, *Chem. Phys.* **123**, 317 (1988).
- ⁵³H. Lefebvre-Brion and R. W. Field, *Perturbations in the Spectra of Diatomic Molecules* (Academic, Orlando, 1986), pp. 375–378.

The Journal of Chemical Physics is copyrighted by the American Institute of Physics (AIP). Redistribution of journal material is subject to the AIP online journal license and/or AIP copyright. For more information, see <http://ojps.aip.org/jcpo/jcpcr/jsp>
Copyright of Journal of Chemical Physics is the property of American Institute of Physics and its content may not be copied or emailed to multiple sites or posted to a listserv without the copyright holder's express written permission. However, users may print, download, or email articles for individual use.

The Journal of Chemical Physics is copyrighted by the American Institute of Physics (AIP). Redistribution of journal material is subject to the AIP online journal license and/or AIP copyright. For more information, see <http://ojps.aip.org/jcpo/jcpcr/jsp>